



## Interface Debonding Detection for an Irregular Complex Multi-chamber Steel Reinforced Concrete Column with PZT Measurements

**B. Xu<sup>1</sup>, Z. Li<sup>2</sup>, S. J. Dyke<sup>3</sup>**

*1 Professor, College of Civil Engineering, Hunan University, Changsha, Hunan 410082, P.R.China.  
E-mail: binxu@hnu.edu.cn.*

*2 Research Assistant, College of Civil Engineering, Hunan University, Changsha, Hunan 410082, P.R.China.  
E-mail: 632436088@qq.com.*

*3 Professor, School of Mechanical Engineering, Purdue University, West Lafayette, IN 47907-2051, USA.  
E-mail: sdyke@purdue.edu.*

### ABSTRACT

Complex steel reinforced concrete (SRC) columns have been extensively adopted as vertical load-carrying structural components in super high-rise buildings. The interface bonding condition between the concrete core and embedded steel plates remain significant concern. The interfacial debonding defect detection is challenging because traditional ultrasonic methods do not work. In this study, a PZT based active interface debonding defect detection approach for multi-chamber SRC columns is proposed and validated experimentally with an irregular multi-chamber SRC specimen. A number of embedded piezo-based functional elements (EPFEs) installed close to the steel plates and piezoelectric ceramic (PZT) patches bonded on the surface of the steel plates are used as actuators and sensors respectively. Based on the amplitude of the measurement of the PZT patches under sinusoidal excitations and the wavelet packet energy under sweep sinusoidal signals, the interface debonding defect are detected successfully. Results show that the amplitude and the wavelet packet energy of the measurement of the PZT sensors in the debonding region are obviously less than in the bonding region. The proposed approach provides a useful way for the interface debonding defect detection of large-scale irregular multi-chamber SRC members in super high-rise buildings.

**KEYWORDS:** *Steel reinforced concrete (SRC), Interfacial debonding detection, Piezoelectric ceramic (PZT)*

### 1. INTRODUCTION

In recent years, a large number of high rise buildings including skyscraper with a design height over 600 meters have been constructed in China. Due to the excellent mechanical performance including high load-carrying capability, good ductility and energy assumption capability under strong dynamic excitations including earthquakes, the steel-concrete hybrid structures including concrete-filled steel tubular (CFST) and steel reinforced concrete (SRC) columns have been extensively adopted as vertical load-carrying structural components in super high-rise buildings. With the increase in the area of the cross section of SRC structures, vertical steel plates in two directions and the steel horizontal diaphragm usually form independent chambers in a single column with an irregular shape. The interface bonding condition between the concrete core and embedded steel plates remain significant concern because of the possible shrinkage of the mass concrete after curing. Research shows that the interface debonding defect can weaken the mechanical properties of components [1].

Even various traditional nondestructive evaluation (NDE) technologies including ultrasound, ground penetration radar, impact echo, and electromagnetic imaging technology have shown their potential for detecting damage in reinforced concrete, their suitability and effectiveness for debonding monitoring of concrete-steel hybrid structures including SRC is still an open research topic. Traditional ultrasonic methods are challenged with the effective detection of interfacial debonding defects due to the irregularity of the specimen. With quick response, high sensitivity, broadband frequency, good linear relationship and other superior characteristics, piezoceramics based method has been widely used in structural health monitoring for reinforced concrete structures and CFST structures. Most early applications of PZT-based damage detection methodologies were based on impedance analysis [2]. Li and Han (2000) presented an approach for the detection of debonding between the steel walls and concrete of CFST members using ultrasonic testing, and the results showed the measured acoustic parameters could reflect the bonding condition [3]. For detecting such damage as voids and debonding between the jacket and the column of fiber reinforced polymer-wrapped concrete structures, Feng et al. (2002) developed an electromagnetic (EM) imaging technology based on the reflection analysis of a continuous EM wave sent toward

and reflected from layered FRP-adhesive-concrete medium[4]. Using the proposed EM imaging technology involving the specially designed and properly installed lenses, the voids and debonding regions were successfully detected. Song et al. (2008) presented a tutorial and a review on the PZT-based smart aggregates (SAs) as multi-functional sensors for concrete structures[5].

For the interface performance monitoring of CFST, PZT based active debonding detection approaches have been proposed using the wavelet packet energy (WPE) or wavelet packet energy spectrum (WPES) of the measurement from PZT patches [6,7]. Results showed that the interface debonding can be detected according to the change in the WPE or WPES of PZT patch measurements. The proposed approach is employed to assess the interface bonding condition of a large cross-section rectangular CFST column of a super high-rise building with a design height of 441.9 meters in China [6]. This proposed interface debonding performance monitoring method provides a novel way for the interface condition evaluation of CFSTs.

In this study, a PZT based active interface debonding defect detection approach for multi-chamber SRC columns is proposed and experimentally validated with an irregular multi-chamber SRC specimen with three independent chambers and artificially mimicked interface debonding defects.

## 2. INTERFACE DEBONDING MONITORING APPROACH

### 2.1 Embedded Piezo-based Functional Elements (EPFEs)

Piezoelectric materials generate electric charge when subjected to a stress or strain (the direct piezoelectric effect) and also produce a stress or strain when an electric field is applied to it in the poled direction (the converse piezoelectric effect). Due to this special piezoelectric property, piezoelectric material can be utilized as both actuators and sensors. In order to monitor the interface condition of SRC members, the PZT actuator should be embedded into the concrete core. Wherefore, in order to protect the brittle piezoelectric transducer from damage, Song et al. (2006) proposed an approach to package a PZT patch to be used as an actuator in a small cement mortar block [8]. Before being packaged in the cement mortar block, the piezoelectric patch is applied with an insulating coating to protect it from the influence of water and moisture. Then the piezoelectric patch is embedded into a 10mm×10mm×10mm cement mortar block to form an embedded piezo-based functional element (EPFE). Figure 2.1 shows the structure of an EPFE to be embedded in the concrete core of the SRC structural members, which can be employed as an actuator to produce stress waves in concrete core. Figure 2.2 shows an example of the EPFE, which is to be used in this study as the actuator.

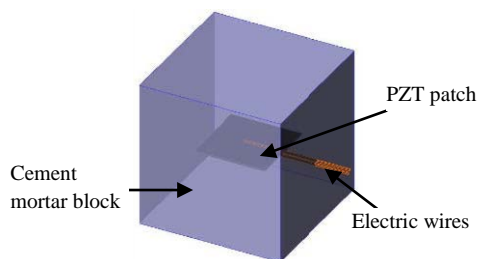


Figure 2.1. Structure of an EPFE



Figure 2.2. Sample of an EPFE

### 2.2 Active Interface Debonding Detection Approach for SRC specimen with PZT

The piezoelectric-based debonding detection method employed in this study is carried out by the analysis on the measurements of PZT patches on the steel plates of the SRC structural members induced by the stress wave propagated from the concrete core. The EPFEs in the concrete core of the SRC column are excited by high frequency signals generated with an arbitrary waveform/function generator and the induced stress wave propagates from concrete core to the steel plates across the interface. Therefore, the outside PZT patches which are employed as sensors patches are excited by the stress waves and produce charges due to the piezoelectric effect, which are recorded with a high speed data acquisition system. The measurements from the PZT sensors patches contain information regarding the interface bonding condition and are used to detect the debonding.

When the stress wave propagates across the interface between the concrete core and the steel plates, it is reflected and scattered at the debonding interface. Therefore, the amplitude and the transmission energy of the corresponding PZT sensors located in the debonding region should be much lower than that of the PZT sensors in bonding region. Therefore, depending on comparison between the amplitude or the energy of the signals output from PZT sensors pasted in the debonding region with that of the PZT sensors pasted in the bonding region, debonding defects of CFST specimen damage can be detected.

### 3. EXPERIMENT STUDY ON INTERFACIAL DEBONDING DETECTION FOR SRC

#### 3.1. Irregular Multi-chamber SRC Specimen

In this paper, an experimental study is conducted on an irregular multi-chamber SRC specimen with three independent chambers and artificially mimicked interface debonding defects. The dimension of the SRC column is 560mm×1200mm×1000mm and the embedded steel plate has a thickness of 10mm made of Q345GJC steel. The specimen before and after casting are shown in Figure 3.1.

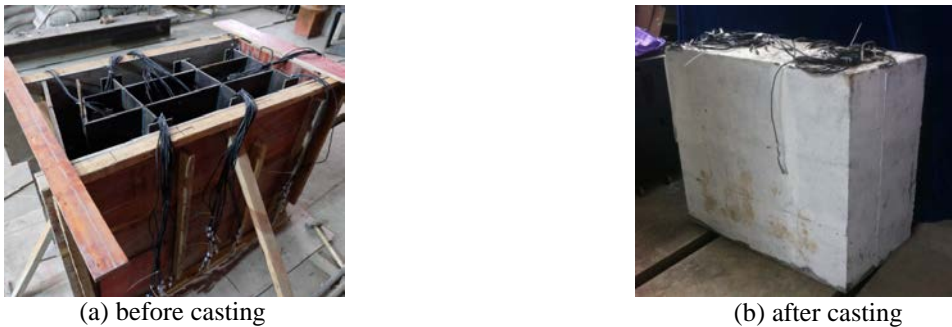


Figure 3.1 Physical figure of the specimen

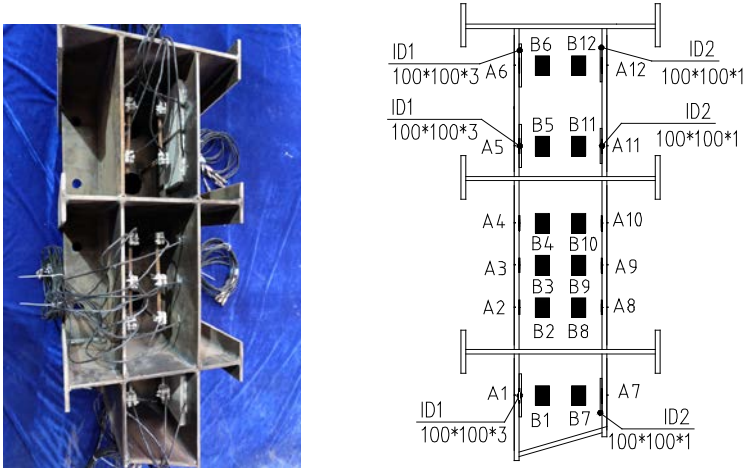


Figure 3.2 Interfacial debonding and PZT and EPFE distribution

Table3.1. Details of the interface scenarios of the irregular multi-chamber SRC specimen

Scenario	Actuators	Sensors	Description
ID1	B1、B5、B6	A1、A5、A6	100mm×100mm×3mm
H	B2、B3、B4	A2、A3、A4	No interfacial debonding
	B8、B9、B10	A8、A9、A10	
ID2	B7、B11、B12	A7、A11、A12	100mm×100mm×1mm

The interfacial debonding (ID) and PZT and EPFE distribution in the specimen are shown in Figure 3.2. Twelve EPFEs installed close to the steel plates and twelve PZT patches bonded on the surface of the steel plates are used as actuators and sensors respectively. There are different interface debonding defects in the specimens. Table 3.1 shows the three interface debonding defects scenarios.

**3.2. Monitoring System**

Figure 3.3 shows the diagram of the monitoring system. The EPFE is excited by output voltage of a sweep sinusoidal signal provided by an arbitrary waveform/function generator to produce the stress waves to propagate in concrete. The PZT sensors receive voltage induced by the stress wave due to the positive piezoelectric effect. In this study, both sinusoidal signals and sweep signals are employed to excite the EPFEs in the irregular multi-chamber SRC specimen. The frequency of the sinusoidal signal is 6kHz, 10kHz, 16kHz, 20kHz and 30kHz, the sweep sinusoidal signal has a frequency range from 1kHz to 20kHz, and the sampling frequency is 102.4kHz. The responses of the PZTs are recorded by the data acquisition system.

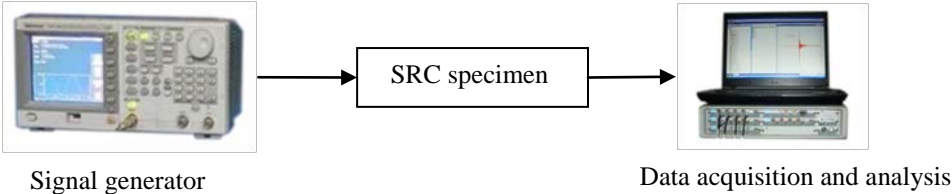


Figure 3.3 Monitoring System

**3.3. Measurements and Analysis**

**3.3.1. Amplitude of PZT measurement under sinusoidal excitations**

Taking the measurement at 10kHz sine signal excitation as an example, Figure 3.4 shows the time domain voltage measurement received by all of the PZT sensors and their corresponding spectrum diagram by Fourier transform. From Figure 3.4(b), it can be seen that the amplitudes of the measurements of PZTs A1, A5 and A6 are close and are the smallest. As shown in Table 3.1, the debonding area corresponding to PZTs A1, A5 and A6 are 100mm by 100mm and the debonding thickness is 3mm. The amplitudes of the measurements of PZTs A7, A11 and A12 are also close to each other and are smaller than them of the PZTs located in the bonding area but greater than them of PZTs A1, A5 and A6. The reason is that the debonding thickness corresponding to the PZTs A7, A11 and A12 is 1mm. It is clear that the amplitude of the measurement of PZT sensor is dependent on the thickness of the debonding.

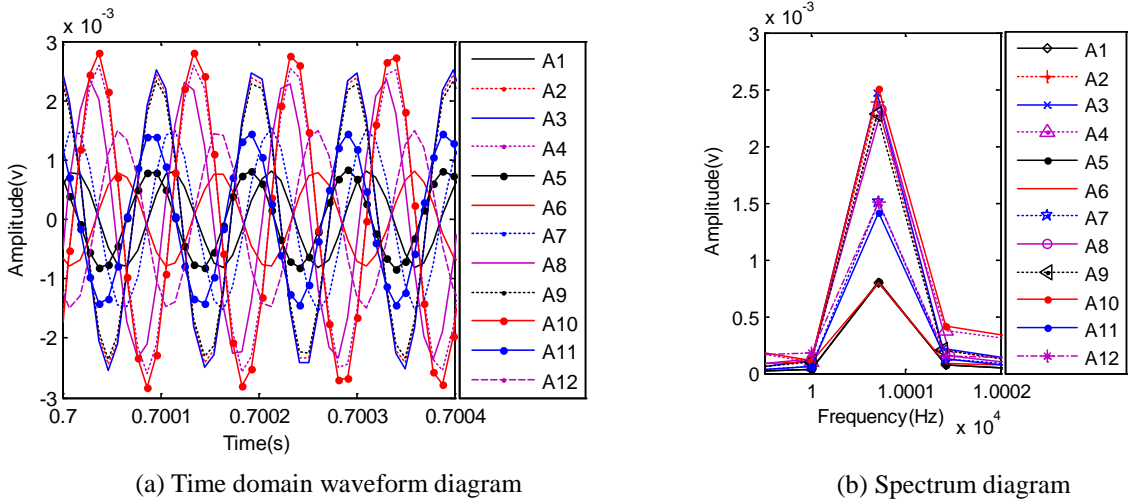


Figure 3.4 Measurement of PZT sensors under sine signal excitation with a frequency of 10kHz

Figure 3.5 shows the average of the sensor signals amplitude under different frequencies when the excitation amplitude is identical. It can be seen that the amplitude of the PZT sensor at bonding location is greater than

others. The average amplitude of the PZT patches at the debonding area with a debonding thickness of 3mm is smaller than that with a debonding thickness of 1mm.

Figures 3.4 and 3.5 show that the amplitude of the measurement of PZT sensor in the debonding region is obviously smaller than that in bonding region. The greater degree of interfacial debonding defect leads to the larger amplitude attenuation.

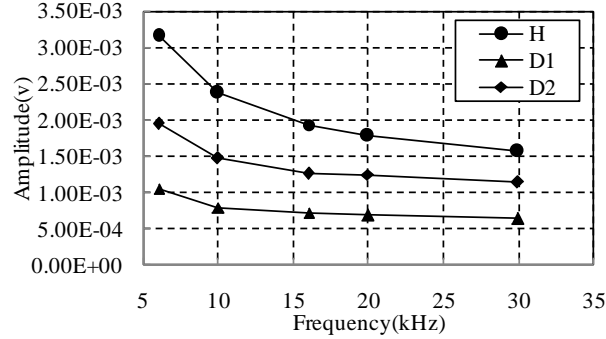


Figure 3.5 The average amplitude of PZTs at different bonding conditions under different frequencies

### 3.3.2. Wavelet packet energy analysis on PZT measurements under sweep signal excitation

The interface debonding detection for the SRC specimen using sweep excitation signals was carried out. In this study, sweep signals of the PZT sensors are analyzed by the wavelet packet decomposition analysis, and an evaluation index is defined based on the wavelet packet analysis on the PZTs measurements. The wavelet packet analysis can further decompose the high-frequency components of original signals thus is more precise than traditional wavelet analysis. Moreover, it can select corresponding frequency band adaptively according to the characteristics of analyzed signal, make it match with the signal spectrum to improve the time-frequency resolution.

First, the signal from each PZT sensor is decomposed by  $N$ -level wavelet packet decomposition into  $2^N$  signal sets as follows,

$$S = [S_1 + S_2 + \dots + S_i + \dots + S_{2^N-1} + S_{2^N}], (i = 1, \dots, 2^N) \quad (3.1)$$

where  $S$  is original signal after filtering and  $s_{2^N}$  is signal after  $N$ -level wavelet packet decomposition.  $s_i$  can be expressed as

$$s_i = [s_{i,1} \quad s_{i,2} \dots s_{i,m-1} \quad s_{i,m}] \quad (3.2)$$

where  $m$  is the number of the sampling data.

The energy vector is expressed as

$$\bar{E} = [e_1 \quad e_2 \quad \dots \quad e_{2^N-1} \quad e_{2^N}] \quad (3.3)$$

where  $e$  is the energy of decomposed signal and can be defined as

$$e_j = \sum_{k=1}^m s_{j,k}^2, (j = 1, \dots, 2^N) \quad (3.4)$$

where  $j$  is the frequency band index.

$$E = \sum_{k=1}^N e_k \quad (3.5)$$

Then, the health index employed in this study can be defined as follows:

$$EI_i = \frac{E_i}{\overline{E_H}}, (i = 1, \dots, n) \quad (3.6)$$

where  $\overline{E_H}$  = the average wavelet packet energy of the sensors under the health condition,  $E_i$  = the wavelet packet energy of each sensor,  $n$  is the number of PZT sensors of monitoring area. When the PZT sensor is located in a debonding area, the corresponding EI will be less than 1.

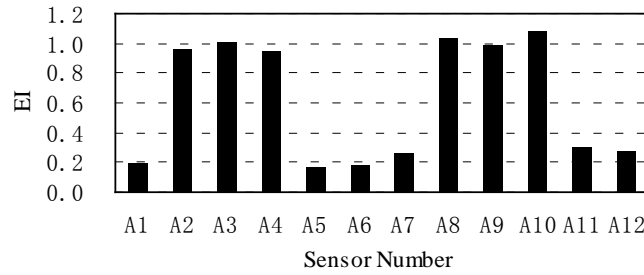


Figure 3.7 Health indices of each sensor

Figure 3.7 show the calculation results of health indices of all of the PZT sensors employed in the test. It is clear that the indices of PZT sensors of A1, A5, A6 and A7, A11, A12 are far less than 1, and the indices of A1, A5, A6 are smaller than that of A7, A11, A12. It is clear that the index defined with the wavelet packet energy is capable of detecting the interface debonding and is related to the degree of interface debonding. The health index becomes smaller with the increase of the thickness of the interfacial debonding defects.

#### 4. CONCLUDING REMARKS

In this paper, a PZT based active interface debonding defect detection approach using embedded piezo-based functional elements (EPFEs) and PZT patches bonded on the surface of the steel plates as actuators and sensors respectively for multi-chamber SRC columns is proposed. The effectiveness of the proposed approach was experimentally verified. The detected interfacial debonding defects have good agreement with the predesigned interfacial debonding defects.

The amplitude of the PZT measurement under sinusoidal excitations and the health index defined by the wavelet packet energy are employed to identify the existence of interface debonding defect and to evaluate the severity of interface debonding defect quantitatively. The location of the interface debonding can be detected successfully and the difference in the evaluation indices corresponding to different level of interface debonding can be found.

Based on the experiment study, the proposed PZT sensing techniques and the corresponding analysis approach have great potential to be applied in practice for the interface debonding defect detection of large-scale irregular multi-chamber SRC members in super high-rise buildings.

#### ACKNOWLEDGEMENTS

The authors gratefully acknowledge the support provided by the National Natural Science Foundation of China (NSFC) under grant No. 51278185 and the Specialized Research Fund for the Doctoral Program of Higher Education (SRFDP) under grant No.20120161110023.

## REFERENCES

1. Tu, G. Y., Yan, D. H., Shao, X. D., et al. (2011). Debonding effects on internal force and stiffness of single tube concrete-filled steel tubular arch rib. *Advanced Materials Research*. **168**,1264-1271.
2. Park, G., Cudney, H.H. and Inman, D.J. (2001). Feasibility of using impedance-based damage assessment for pipeline structures. *Earthquake Engineering and Structural Dynamics*. **30**,1463-1474
3. Li, L.Q. and Han, X.J. (2003). Using ultrasonic method to examine the quality of CFST. *Journal of Nanjing Architectural and Civil Engineering Institute*. **53**,26-32
4. Feng, M. Q., Flaviis, F. De, and Kim, Y. J. (2002). Use of microwaves for damage detection of FRP-wrapped concrete structures. *Journal of Engineering Mechanical ASCE*.**128**:2,172-183
5. Song, G., Gu, H., and Mo, Y.L., (2008). Smart aggregates: multi-functional sensors for concrete structures-A tutorial and a review. *Smart Materials and Structures*. **17**:3,033001
6. Xu, B., Li, B., Song, G. (2012). Active debonding detection for large rectangular CFSTs based on wavelet packet energy spectrum with piezoceramics. *ASCE Journal of Structural Engineering*. **139**:9,1435-1443.
7. Xu, B., Zhang, T., Song, G., et al. (2013). Active interface debonding detection of a concrete-filled steel tube with piezoelectric technologies using wavelet packet analysis. *Mechanical Systems and Signal Processing*. **36**:1,7-17.
8. Song, G., Gu, H., Dhonde, H., Mo, Y.L. and Yan, S. (2006). Concrete early-age strength monitoring using embedded piezoelectric transducers. *Smart Materials and Structures*. **15**, 1837-1845.